REPORT No. 502

SCALE EFFECT ON CLARK Y AIRFOIL CHARACTERISTICS FROM N.A.C.A. FULL-SCALE WIND-TUNNEL TESTS

By Abe Silverstein

SUMMARY

Tests were conducted in the N.A.C.A. full-scale wind tunnel to determine the aerodynamic characteristics of the Clark Y airfoil over a large range of Reynolds Numbers. Three airfoils of aspect ratio 6 and with 4-, 6-, and 8-foot chords were tested at velocities between 25 and 118 miles per hour, and the characteristics were obtained for Reynolds Numbers (based on the airfoil chord) in the range between 1,000,000 and 9,000,000 at the low angles of attack, and between 1,000,000 and 6,000,000 at maximum lift. With increasing Reynolds Number the airfoil characteristics are affected in the following manner: The drag at zero lift decreases, the maximum lift increases, the slope of the lift curve increases, the angle of zero lift occurs at smaller negative angles, and the pitching moment at zero lift does not change appreciably.

The Clark Y airfoil characteristics obtained from the tests in the full-scale tunnel are compared with those from the variable-density and the propeller-research tunnels, and with the theoretical values. An analysis of the comparative experimental data indicates that the air stream of the full-scale tunnel has a relatively low turbulence. This inference is substantiated by the close agreement obtained between the characteristics of airplanes measured in the full-scale tunnel and those from flight tests, and by sphere drag measurements that show the tunnel has a turbulence similar to free air. It is therefore believed that the effects of turbulence on the characteristics of an airfoil tested in the full-scale tunnel are small, and may be neglected in applying the data to design.

INTRODUCTION

The aerodynamic characteristics of airfoils ascertained from different wind-tunnel investigations are frequently not in agreement. The reasons for these discrepancies are generally understood, having been revealed partly by theory and partly through experiment. The complete force equation, which includes the terms expressing dynamic similitude, shows theoretically that comparable wind-tunnel results should be obtained when airfoils having similar surfaces are tested at the same Reynolds Number in wind tunnels with like turbulences. Experimental research has indicated, however, that it is unusual to obtain the same results from several tunnels, even when these fundamental similitude requirements are satisfied. Some of the more important sources of experimental discrepancies are wind-tunnel boundary interference, airfoil-support interference, and air-stream irregularities and asymmetries.

As a result of the failure of wind-tunnel testing to fulfill the exacting requirements of similarity in both the flow and the test procedure, disagreements occur in published results purporting to give the experimentally obtained characteristics of airfoils of the same section. These conflicting results from tests in numerous wind tunnels confront the designer with an arduous task. The variety of data must not only be analyzed and interpreted for application to the particular design problem, but it must also be extrapolated to flight Reynolds Number. This extension of the data has usually been necessary because experimental information has not been available above a Reynolds Number of about 3,000,000, whereas the flight range lies between 2,000,000 and 25,000,000. There is no exact and rational method for making a transformation from the best wind-tunnel information to the desired flight characteristics, although experience serves as a useful guide.

With the idea of helping the designer to span this gap between small-tunnel information and flight conditions the study of airfoil characteristics has been continued in the N.A.C.A. full-scale wind tunnel. Here unique equipment is available for testing large size airfoils at Reynolds Numbers comparable with those of flight. The full-scale tunnel has a further advantage over smaller tunnels in that the full-scale-tunnel data on airplanes may be directly compared with those obtained in flight tests, thus disclosing any disturbing tunnel effects and checking the wind-tunnel testing conditions and technic.

Tests were therefore made in the tunnel to determine the aerodynamic characteristics of the Clark Y airfoil over a large range of Reynolds Numbers. By tests of airfoils with the same aspect ratio and chords of 4, 6, and 8 feet at velocities from 25 to 118 miles per hour, the characteristics were investigated over a Reynolds

Number range from about 1,000,000 to 9,000,000, although data were not secured above a Reynolds Number of about 6,000,000 at maximum lift. A portion of these results was used in an experimental verification of the theoretical jet-boundary correction for the elliptical-jet wind tunnel which has been reported in reference 1.

FIGURE 1.—The 6 by 36 airfoil mounted in the full-scale tunnel.

EQUIPMENT AND AIRFOILS

The N.A.C.A. full-scale wind tunnel and equipment are described in reference 2. Since the general equipment and apparatus used in these tests were essentially the same as reported in the aforementioned reference, a further description will not be given.

During the tests the airfoils were mounted in the jet, as shown in figure 1, on supports that attach to the airfoils at the one-quarter-chord point, and transmit the forces to the balance below. The small diagonal streamline arms connected to the rear of the airfoil serve to change the angle of attack by pivoting it about the main support pins. The lower ends of these diagonal arms are attached to screw mechanisms by means of which the angle is adjusted to within $\pm 0.05°$. The fairings over the airfoil supports are not connected to the balance but are independently supported at the balance-house roof. The short exposed upper portions of the main supports have Navy no. 1 strut sections, and taper to a cross section of about 1 by 3 inches where they connect to the airfoil.

Three metal Clark Y airfoils with 4-, 6-, and 8-foot chords and of aspect ratio 6 were used. The airfoil covering of $\frac{1}{16}$-inch aluminum sheet was attached to a rigid internal structure by means of flush countersunk screws. The spars were steel beams and the profile was formed by aluminum ribs spaced at 12-inch intervals. Access to the airfoil support pins was provided by removable plates which were screwed flush with the surface during the tests. Tapped openings for fitted eyebolts were spaced over the airfoil for attachments when taking tare measurements. Flush screw plugs

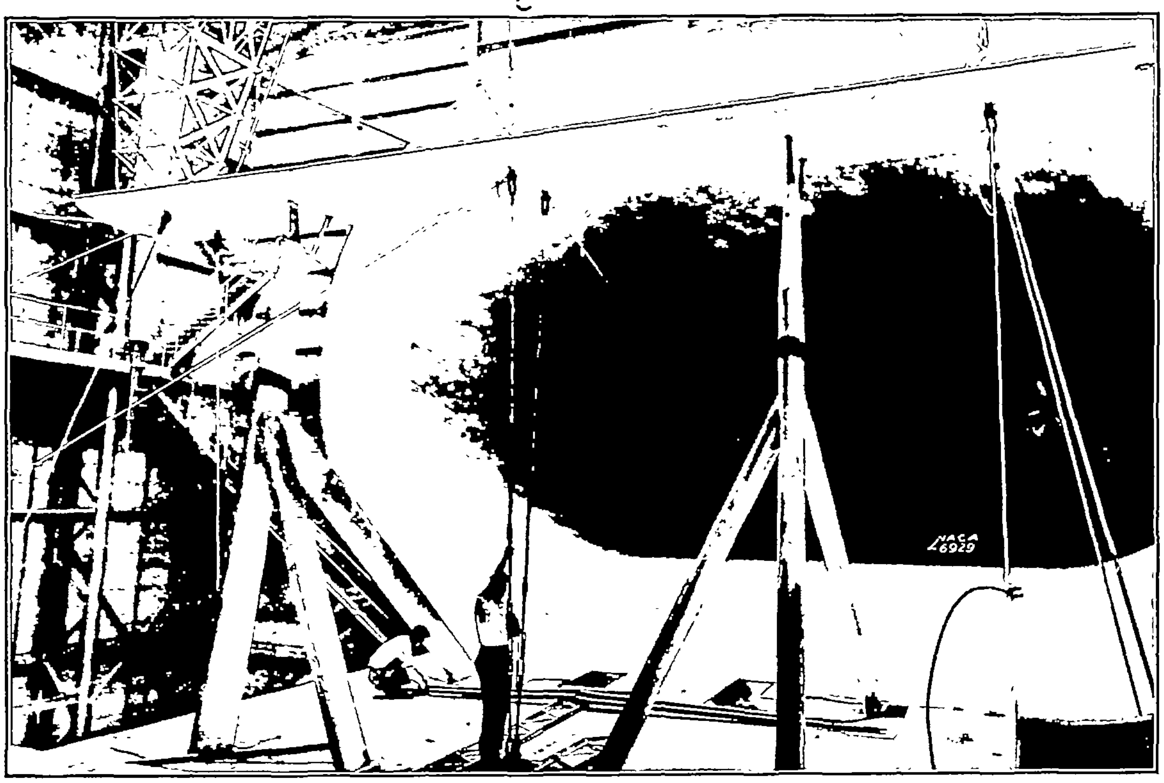

FIGURE 2.—A tare-force set-up with inverted 6 by 36 airfoil.

were inserted in these openings during the regular force tests. The smooth aluminum surfaces of the airfoil were covered with a protective coat of varnish. The airfoils were manufactured under careful inspection so as to maintain the specified ordinates, and were accurately measured just before testing. The specified and measured ordinates are given in table I. No appreciable twists, deformations, or local irregularities changed the airfoil accuracy during the period of the tests.

TESTS

The lift, drag, and pitching moments were measured at six speeds between 25 and 118 miles per hour over a range of angles of attack from $-8°$ to $24°$. These tests were made with the airfoils in an upright position in the tunnel, and then repeated through an angle range of $-8°$ to $5°$ with the airfoils inverted.

Tare forces on the supports were measured with the airfoils in the test position but supported independently of the regular supports and rigidly held in place by auxiliary cables (fig. 2). The tare-force measurements therefore include the interference of the airfoils upon the supports. Tare forces were measured for all the airfoils at five angles of attack and at all test speeds.

The interference of the supports upon the 8 by 48 airfoil was ascertained by adding duplicate supporting struts to the normal installation (fig. 3). As these dummy struts were not connected to the airfoil or balance, any changes in the measured characteristics with the struts in place could be attributed to their interference. A similar method was employed for the tests of the 4 by 24 airfoil using, however, only a single dummy support and doubling the interference effect when applying the results to the airfoil. Interference drag for the 6 by 36 airfoil was interpolated from data on the other two airfoils.

Static and dynamic pressure surveys were made several chord lengths ahead of the 4 by 24 and 8 by 48 airfoils to determine the blocking effect of the airfoils upon the tunnel stream. These surveys were made at a number of angles of attack between zero and maximum lift. For the 6 by 36 airfoil the blocking effect was interpolated from data on the other two airfoils.

CORRECTION OF DATA

The uncorrected lift and drag forces on the airfoils were measured on recording scales, and the pitching moment was computed by multiplying the lift and drag forces by the proper lever arms. The observed wind-tunnel data were then corrected in the following manner:

(*a*) The first process in correcting the data was to adjust the measured dynamic pressures. The dynamic pressure of the wind-tunnel jet is measured with a manometer, which indicates the pressure difference between the return passage and the test chamber (reference 2). The dynamic pressure in the jet is obtained by a calibration. Previous study has shown that this indicated velocity head, obtained from a calibration with no body in the jet, is in error owing to the blocking action of the body in the air stream. The blocking increases with the angle of attack; the Reynolds Numbers of the tests are therefore slightly different at the low and high angles of attack. A full discussion of the correction as applied to the airfoil data is given in reference 1. The magnitude of

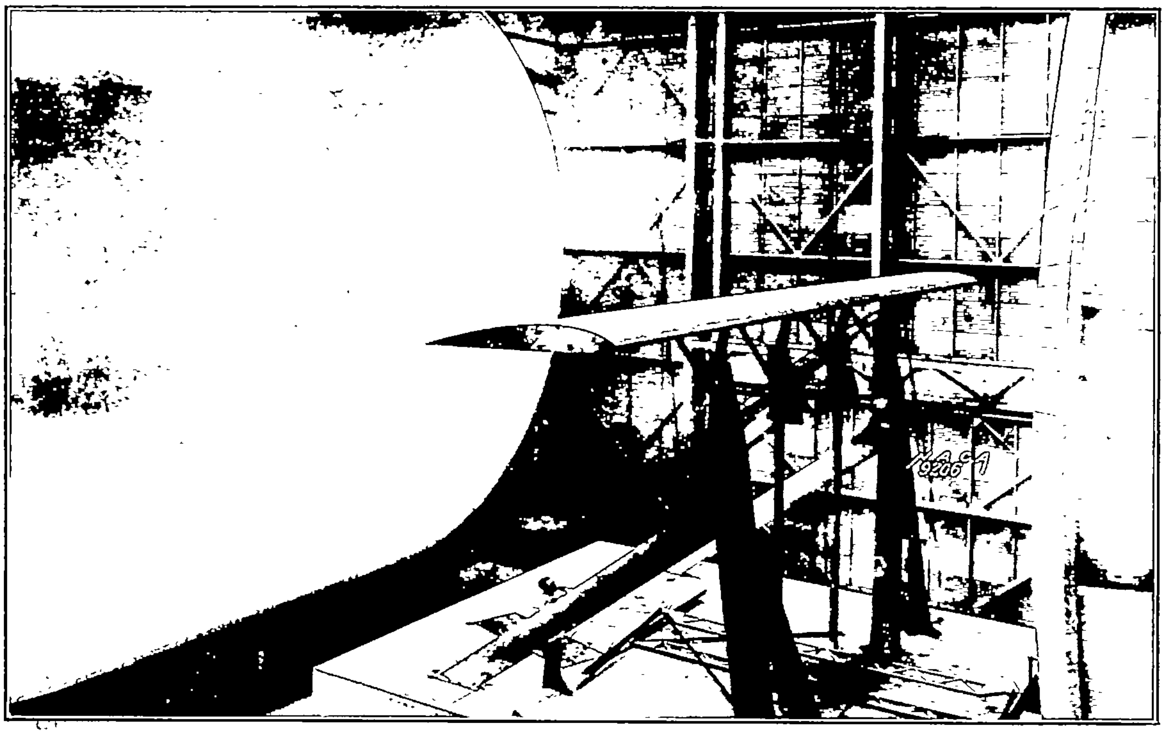

FIGURE 3.—Dummy supports added to the 8 by 48 airfoil set-up for interference tests.

the blocking effect of the three airfoils is shown in figure 4.

(*b*) Tare force and moment coefficients were then computed and deducted from the gross force coefficients to obtain net values. The tare drag is about 2 percent of the minimum drag for the 8 by 48 airfoil

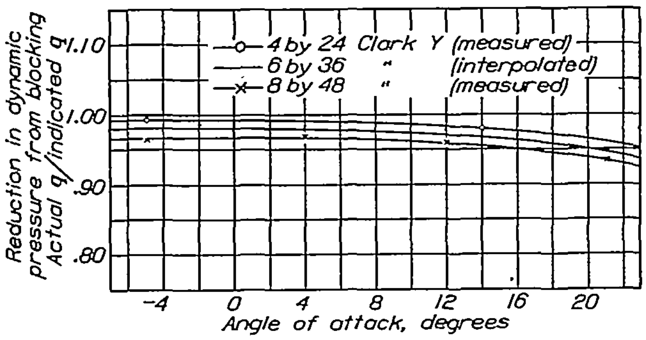

FIGURE 4.—Blocking corrections for the three airfoils tested in the full-scale tunnel.

and 10 percent of the minimum drag for the 4 by 24 airfoil. The tare lifts and moments are negligible.

(*c*) Interference effects of the struts on the airfoils were then included. Figure 5 illustrates the interference caused by two struts on the lower surface of the 8 by 48 airfoil. The effect on the drag is quite

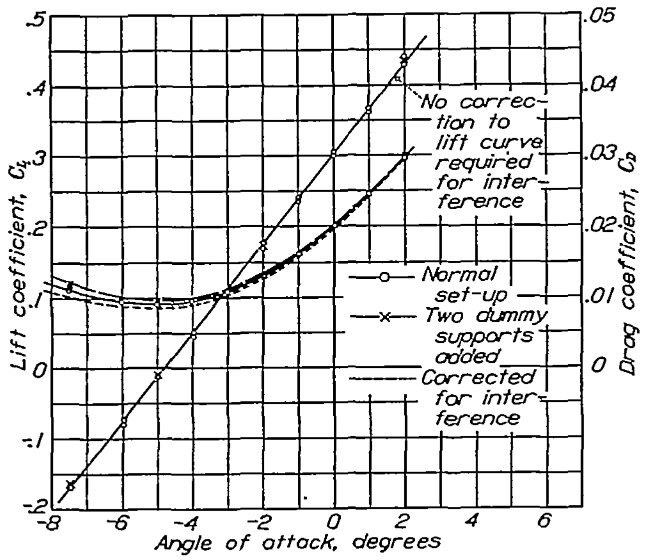

FIGURE 5.—The effect of strut interference on the characteristics of the 8 by 48 Clark Y airfoil when tested upright. Reynolds Number, 6.12×10^6.

large in the region of zero lift, but decreases and becomes negligible at higher lift coefficients. The interference effect on the lift is negligible and within the experimental error.

The support interference on the 4 by 24 airfoil had an effect similar to changing the camber of the airfoil. The angle of zero lift was changed by the interference when the airfoil was tested both in the upright and inverted positions. A comparison of the measured drag values at zero lift, with and without the dummy support struts, showed that the supports exerted a large unfavorable interference in the upright tests, and a slightly favorable one when the airfoil was inverted. In all cases for the upright tests the effects became very small on both drag and lift above a lift coefficient of 0.3.

(*d*) Upright and inverted tests on the airfoils indicated that the air stream had an initial downflow angle; it was necessary to correct the characteristics for this effect. In order to determine the magnitude of the air-stream angle, plots were made of the D/L against C_L for the upright and inverted airfoil tests (fig. 6). The D/L ordinate between the two curves is equal to 2 sin β, where β is the air-stream angle. A check on the air-stream angle is possible by noting the separation of the upright and inverted lift curves.

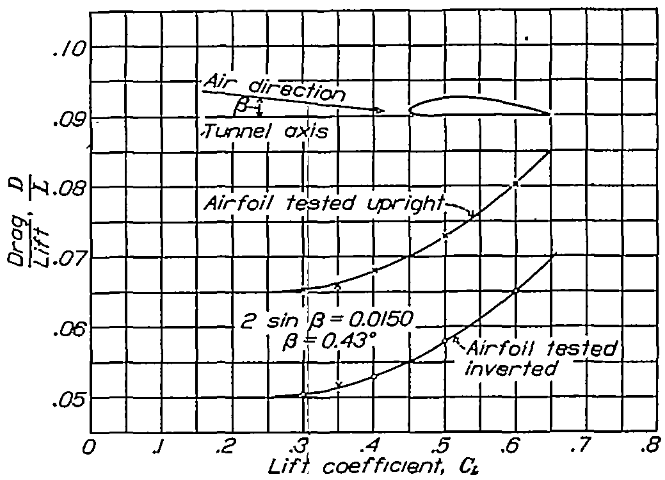

FIGURE 6.—Method of obtaining air-stream angles from upright and inverted tests. Reynolds Number, 6.12×10^6; 8 by 48 airfoil.

Since the separation of the upright and inverted lift curves, when plotted as values of C_L against α, is due to the air-stream angle, the value of the air-stream deflection is equal to one-half the angle between the two curves. If the interference effects are not properly accounted for, the values of the air-stream angle, from the two methods, will not agree. The angles determined by these two methods generally agreed within about 0.1°. The average value was taken as the true air-stream angle, although no rational excuse can be offered for this practice, except that the probable percentage of error is reduced.

(*e*) The limited boundaries of the wind-tunnel jet are a source of error in ascertaining the characteristics of any body tested therein. A correction for this boundary interference was therefore applied to the airfoil angle of attack and the drag coefficient. For these tests the correction factor was determined experimentally by an extrapolation of the airfoil data to free air values. A complete description of this method with the values of the experimental and theoretical corrections[1] is given in reference 1.

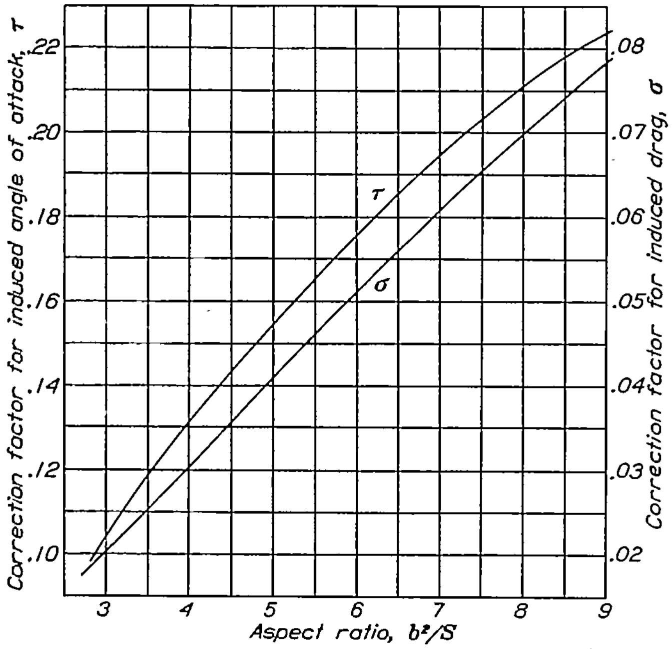

FIGURE 7.—Correction factors for transforming rectangular airfoils from finite to infinite aspect ratio.

(*f*) The corrected characteristics for the airfoils with aspect ratio 6 were then transformed into infinite-aspect-ratio characteristics by the following formulas:

$$\alpha_0 = \alpha - \frac{C_L}{\pi R}(1+\tau)\ 57.3$$

$$C_{D_0} = C_D - \frac{C_L^2}{\pi R}(1+\sigma)$$

where

α_0 is the angle of attack in degrees at which an airfoil with infinite span would give the same lift coefficient as the airfoil tested in the tunnel.

C_{D_0}, the profile-drag coefficient.

R, the aspect ratio.

τ, a factor correcting the induced angle of attack, to allow for the change from elliptical span loading to one resulting from the use of an airfoil with rectangular plan form.

σ, a factor correcting the induced drag, to allow for the change from elliptical span loading to one resulting from the use of an airfoil with rectangular plan form.

and where α, C_L, and C_D, are the corrected characteristics for finite aspect ratio. The angle of attack, α, is in degrees. Values of τ and σ are taken from figure 7, and are based on the assumptions of a theoretical rectangular loading, and a value of 0.101 for the slope of the infinite-aspect-ratio lift curve. Experimentally the rectangular airfoils did not have a loading identical to the theoretical, owing to jet-boundary effects and velocity asymmetries. This variation would require the use of values for σ and τ slightly larger than those in figure 7. Since results were not available to indicate

[1] The corrections reported in this reference were from the results of tests at a Reynolds Number of 2,000,000. When the complete results of the airfoils at all Reynolds Numbers were analyzed it was found that values were obtained for the jet-boundary correction which were slightly different from those reported, and approached even more closely the theoretical values given in reference 1. These corrected factors have been applied to the present data.

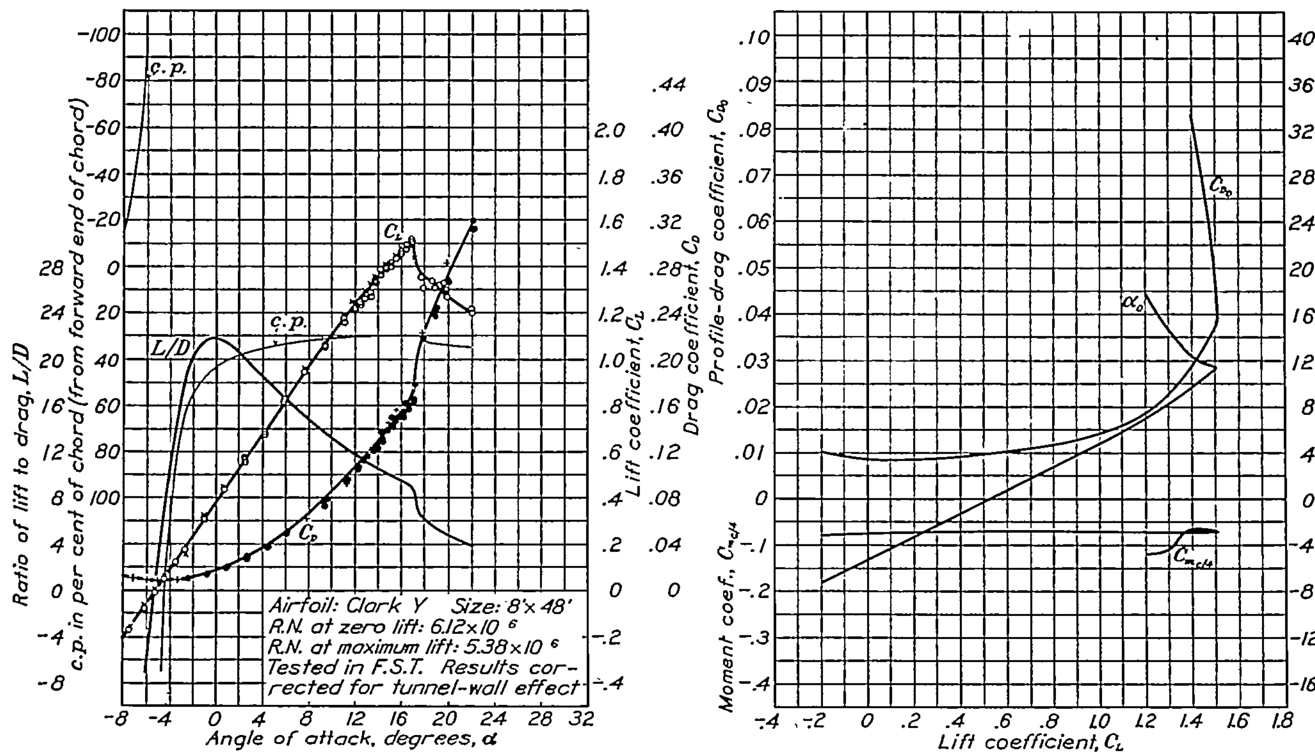

FIGURE 8.—Characteristics of the 8 by 48 Clark Y airfoil at a Reynolds Number of about 6,000,000.

the pressure distribution over the airfoils in the tunnel, this effect, which is small in magnitude, is not included.

RESULTS

The corrected results are tabulated giving values of C_L, α, C_D, L/D, and $c.p.$ for the Clark Y airfoil with aspect ratio 6, and values of α_0, C_{D_0}, and C_m for the airfoil with infinite aspect ratio. These data for the three airfoils at all Reynolds Numbers tested are presented in tables II to XX, inclusive. Values of $c.p.$ are given in percent chord. A typical plot of the data from table XVIII is given in figure 8.

The curves summarizing variations of the principal airfoil characteristics with Reynolds Number are of

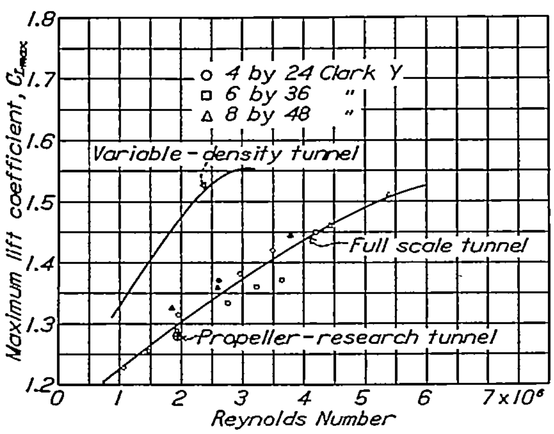

FIGURE 9.—Variation with Reynolds Number of maximum-lift coefficients for the Clark Y airfoil. Propeller-research-tunnel value from reference 3. Variable-density-tunnel data from reference 4.

particular interest. Figure 9 shows the variation of the maximum lift coefficient for the Clark Y airfoil over a Reynolds Number range from 1,000,000 to 6,000,000. In this figure the results of Clark Y tests

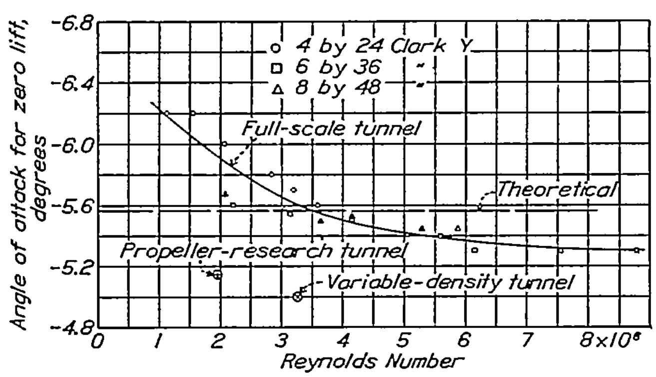

FIGURE 10.—Variation with Reynolds Number of the Clark Y angle of attack at zero lift. Propeller-research-tunnel value from reference 3. Variable-density-tunnel value from reference 4. Theoretical value from reference 5.

in the N.A.C.A. variable-density wind tunnel over a range from 1,000,000 to 3,000,000 are also given. A single point gives the maximum lift obtained on the Clark Y airfoil in the propeller-research tunnel at a Reynolds Number of about 2,000,000. Figure 10 covers the change in the angle of attack for zero lift with Reynolds Number. Results from the variable-density and propeller-research tunnels, as well as a

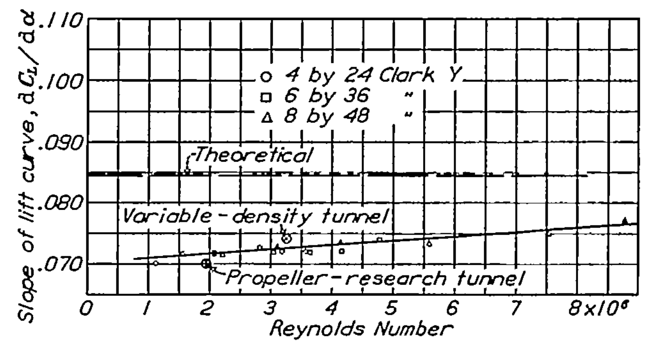

FIGURE 11.—Variation with Reynolds Number of the slope of the lift curve for the Clark Y airfoil (slope for an airfoil of aspect ratio 6; α in degrees). Propeller-research tunnel value from reference 3. Variable-density-tunnel value from reference 6. Theoretical value from reference 5.

theoretical value from reference 5, are also included on this figure. In a similar manner, figure 11 presents the change in slope of the lift curve with scale. The

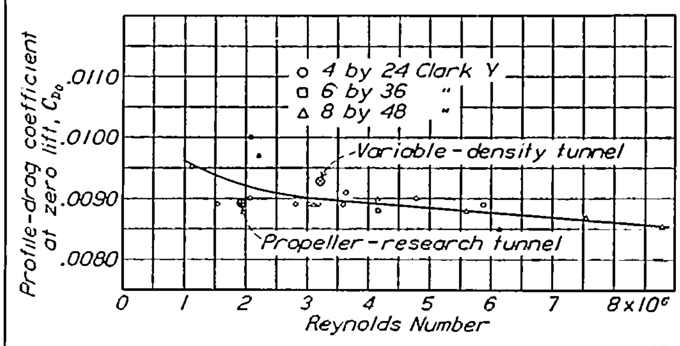

FIGURE 12.—Variation with Reynolds Number of the Clark Y profile-drag coefficient at zero lift. Propeller-research-tunnel value from reference 3. Variable-density-tunnel value from reference 6.

airfoil profile-drag coefficient at zero lift is shown on figure 12 over a Reynolds Number range from 1,000,000 to 9,000,000, and values from the variable-density and

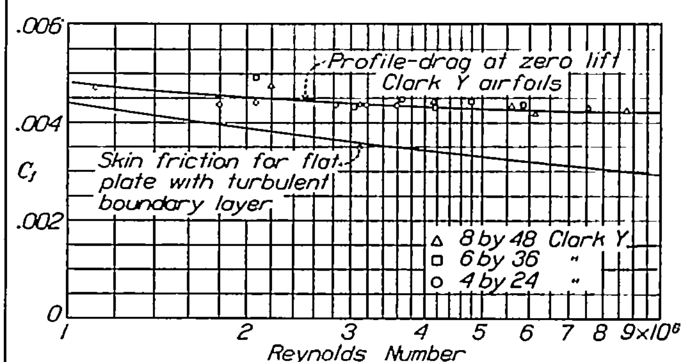

FIGURE 13.—Comparison of the Clark Y profile-drag coefficient at zero lift with the skin-friction drag coefficient for a flat plate having a completely turbulent boundary layer. C_f for airfoils based on actual surface area.

the propeller-research tunnels are again included. In figure 13 the profile-drag coefficient at zero lift for the airfoil is compared with the skin-friction drag coefficient for a flat plate with turbulent boundary layer.

Curves in figure 14 represent the profile-drag coefficient at C_L values of 0.1 and 0.2 plotted against Reynolds Number. The variation of pitching-moment coefficient at zero lift and the maximum value of L/D are plotted against the Reynolds Number in figures 15 and 16, respectively.

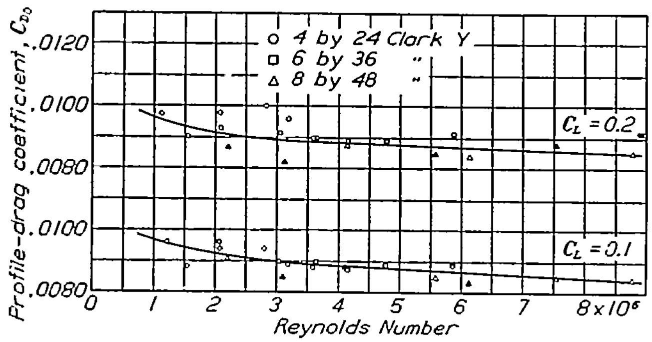

FIGURE 14.—Variation with the Reynolds Number of the Clark Y profile-drag coefficient at lift coefficients of 0.1 and 0.2.

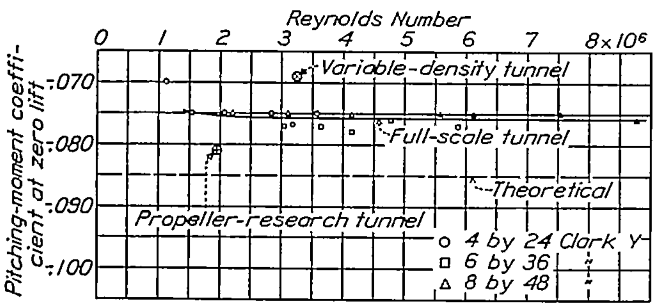

FIGURE 15.—Variation with Reynolds Number of the Clark Y pitching-moment coefficient at zero lift. Propeller-research-tunnel value from reference 3. Variable-density-tunnel value from reference 6. Theoretical value from reference 5.

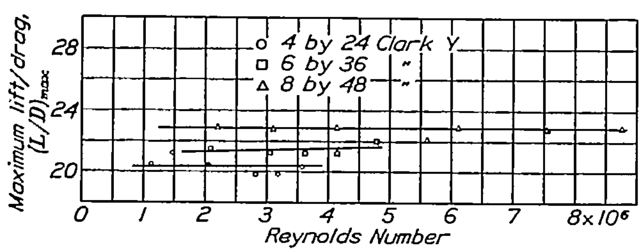

FIGURE 16.—Variation with Reynolds Number of the maximum value of L/D for the Clark Y airfoil.

PRECISION

The number of variables involved makes the precision of all wind-tunnel results exceedingly difficult to estimate. The reference for gaging the precision of wind-tunnel airfoil results should be *the characteristics which the specified airfoil would have in flight at the particular Reynolds Number*. Wind-tunnel results would then include accidental errors of measurement, errors in the application of wind-tunnel interferences, and variations of the characteristics due to differences in airfoil accuracy and turbulence. If the turbulence is considered as a parameter with which characteristics vary rather than as a source of error in precision, the reference base may be changed to *the hypothetical characteristics which the airfoil would have in free air at the same Reynolds Number and turbulence*. This attitude has been adopted in considering the accuracy of the results found in this investigation.

The exactness with which the final precision may be predicted depends upon the thoroughness with which the following factors are known:

(*a*) Regularity and accuracy in measuring air-stream velocity and angularity.

(*b*) Rigidity of airfoil supports and accuracy of setting the angle of attack.

(*c*) Accuracy of balance readings.

(*d*) Accuracy of the airfoils.

(*e*) Accuracy of measured support interferences.

(*f*) Accuracy of the applied jet-boundary correction.

Repeat runs indicated that the accidental errors, such as are to a large extent included in (*a*), (*b*), and (*c*) of the foregoing, were small, and within the following limits:

$$\alpha = \pm 0.05°$$
$$C_{L_{max}} = \pm 0.01$$
$$\frac{dC_L}{d\alpha} = \pm 0.001 \text{ per degree}$$
$$C_{D_0} = \pm 0.0002 \ (C_L = 0)$$
$$C_{D_0} = \pm 0.0010 \ (C_L = 1)$$
$$C_{m_{c/4}} = \pm 0.001$$

A deflection of the airfoil supports introduces an error into the pitching-moment coefficients. In these tests, however, the strong tripod type of construction used in the airfoil supports and the relatively short cantilever section reduced deflections to negligible amounts. Errors from this source may therefore be disregarded.

It was found impossible to evaluate the loss in precision due to differences between the specified and measured airfoil ordinates. Variable-density-tunnel tests have shown that small errors in the nose profile of model airfoils are quite critical, while differences farther back along the chord are not of great importance. From an examination of table I, it may be seen that the airfoils were not constructed exactly in accordance with the specified ordinates, and that there were small differences between measured and specified ordinates at the airfoil nose; the surfaces, however, were fair in all cases. The lack of any serious systematic disagreement in the results from the several airfoils indicates that errors from this source were not large enough to be significant.

The experimentally derived values of wind-tunnel and support interference were subject to the same accidental and inherent errors as the tests proper, but these errors would have only a secondary effect on the final results. From a consideration of all the contributing errors the estimated final precision is as follows:

$$\alpha = \pm 0.1°$$
$$C_{L_{max}} = \pm 0.03$$
$$\frac{dC_L}{d\alpha} = \pm 0.0015 \text{ per degree}$$
$$C_{D_0} = \pm 0.0004 \ (C_L = 0)$$
$$C_{D_0} = \pm 0.0015 \ (C_L = 1.0)$$
$$C_{m_{c/4}} = \pm 0.003$$

DISCUSSION

Lift.—The maximum lift coefficient, the angle of zero lift, and the slope of the lift curve for the Clark Y airfoil vary with the Reynolds Number (figs. 9, 10, and 11). Perhaps of greatest interest because of their significance in regard to the question of turbulence are the maximum lift coefficients, particularly in comparison with those from the variable-density tunnel (reference 4) and the value from the propeller-research tunnel (reference 3) shown in figure 9. There is an excellent agreement between the value of the maximum lift coefficient from the propeller-research tunnel and the full-scale tunnel at a Reynolds Number of about 2,000,000; however, the variable-density-tunnel results are from 10 to 13 percent higher than those from the full-scale tunnel at the same Reynolds Numbers. This difference between variable-density and full-scale-tunnel maximum lift coefficients is believed to be largely due to the unlike turbulences in the two tunnels; the agreement with the propeller-research tunnel suggests that it has the same turbulence as the full-scale tunnel.

Several experimenters have shown that one of the effects of turbulence on medium-cambered medium-thick airfoils, such as the Clark Y, is to increase the maximum lift coefficient. This beneficial effect of turbulence is attributed to the mixing and eddying flow in the turbulent boundary layer around the airfoil, which provides for a larger transfer of momentum from the general flow to the boundary layer than is possible in a laminar stream. When changing from laminar to turbulent flow, the augmented momentum in the boundary layer serves to move the separation point of the flow rearward along the upper surface of the airfoil. This rearward motion allows the airfoil to attain a higher angle of attack and lift coefficient before the separation point moves forward again, with increasing angle, to the point at which the general flow breaks down. A complete discussion of this phenomenon is given in reference 7, and the results of tests included in this reference show that it is possible to increase the lift coefficient of an N.A.C.A. 2412 airfoil as much as 30 percent by the introduction of turbulence. Earlier tests in the variable-density tunnel (reference 4) on the effects of turbulence on a Clark Y airfoil gave similar results. It may therefore be stated that the comparatively low values of maximum lift coefficients in the full-scale tunnel signify a small turbulence. Results of other tests indicate the existence of a turbulent condition in this tunnel similar to that in free air. The critical Reynolds Number for a sphere investigated in the full-scale tunnel (fig. 17)

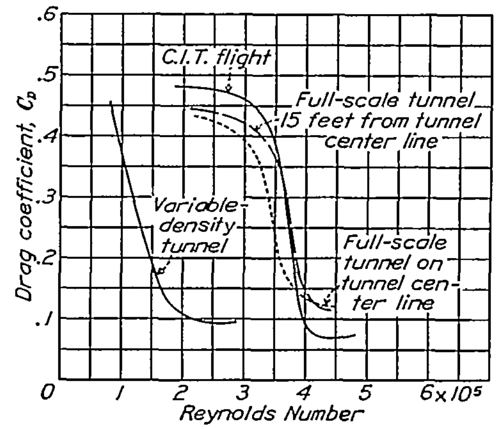

FIGURE 17.—Sphere drag coefficients obtained from flight and wind-tunnel tests. Critical Reynolds Number occurs at C_D equals 0.3. Flight results from reference 8. Variable-density-tunnel results from reference 4.

agrees closely with the critical value obtained in flight (reference 8). Based on the method of Dryden (reference 9), the turbulence in the full-scale tunnel is about 0.35 percent, which value is almost identical with the value obtained by measurements in free air. The critical Reynolds Number in the variable-density tunnel (reference 4) indicates a turbulence of about 2.5 percent.[2]

The good agreement between full-scale tunnel and flight characteristics on airplanes presents further evidence of the small effects of turbulence on the wind-tunnel measurements. The following tabulated data illustrate the comparison between wind tunnel and flight results.

COMPARISON OF FULL-SCALE WIND TUNNEL AND FLIGHT RESULTS ON SEVERAL AIRPLANES

Airplane	Approximate Reynolds Number	Source of results	[1] $C_{L_{max}}$	[1] $C_{D_{min}}$
Martin XBM-1	3,000,000	Full-scale tunnel		0.065
Do	5,000,000	do		.064
Do	13,000,000	Flight		.062
Fairchild F-22	3,500,000	Full-scale tunnel	1.40	.058
Do	3,500,000	Flight	1.36	
Do	6,000,000	do		.058
Boeing PW-9	3,500,000	Full-scale tunnel	1.19	.054
Do	3,500,000	Flight	1.21	
Do	7,000,000	do		.053

[1] The missing values were not measured.

In all cases the checks are within the experimental limits of accuracy. An appreciable change of minimum drag coefficient with Reynolds Number is to be observed in the case of the XBM-1, where the

[2] Slight modifications have been made to the variable-density tunnel since these turbulence measurements were made.

Reynolds Number reached in flight is considerably higher than those of the tunnel.

The experimental evidence suggests that the turbulence of the full-scale tunnel is small and exerts only a negligible effect on the characteristics of bodies tested.

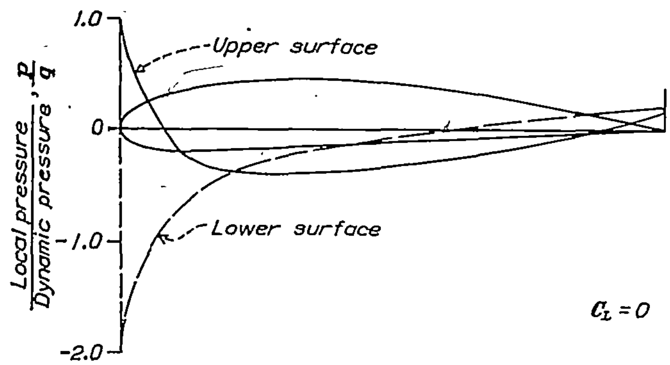

FIGURE 18.—Theoretical pressure distribution on a Clark Y airfoil at the angle of zero lift. Reproduced from reference 5.

The change in the angle of zero lift with Reynolds Number (fig. 10) is, to a large extent, a phenomenon similar to the variation of maximum lift. The angle of zero lift occurs at smaller negative angles with increasing Reynolds Number. This phenomenon can be explained by reference to the pressure distribution over the airfoil for the zero-lift condition (fig. 18). Owing to the large adverse gradient of pressure at the forward portion of the lower surface of the airfoil (a condition similar to that on the upper surface at maximum lift) the stability of the flow is critical; at low Reynolds Numbers there is an early breakdown of this flow. This large adverse pressure gradient not only causes an early breakdown of the flow, but also results in an earlier separation of the flow, which reduces the slope of the lift curve in the range of zero lift, and requires that the airfoil be turned to a larger negative angle to reach zero lift. With large Reynolds Numbers and considerable initial turbulence the breakdown of flow is delayed so that zero lift is reached at smaller negative angles. The smaller negative angles of zero lift from the more turbulent variable density tunnel tests shown in figure 10 agree well with this conception. The experimental value for the angle of zero lift from the full-scale wind tunnel agrees with the theoretical value (reference 3) at a Reynolds Number of 3,500,000.

The slope of the lift curve (fig. 11) shows a constant increase with Reynolds Number. The experimental slope varies from about 85 to 90 percent of the slope theoretically predicted in reference 5. The slope of the lift curve, obtained from the variable density tunnel tests on an airfoil of this thickness (reference 6), at a Reynolds Number of 3,000,000 is slightly greater than the value found in the present tests, whereas the propeller research tunnel value is slightly less. Increased turbulence for the Clark Y may have the same effect upon the lift-curve slope as increased Reynolds Number, which might explain the slightly higher variable density tunnel result.

Drag.—Figure 12 indicates that the profile-drag coefficient at zero lift for the Clark Y airfoil decreases rapidly between the Reynolds Numbers of 1,000,000 and 3,000,000, and then decreases at a constant but much lower rate over the range between 3,000,000 and 9,000,000. The considerable scattering of the experimental points at the lower Reynolds Numbers may possibly be accounted for either by the decreased precision in measuring the extremely small forces or by the uncertain nature of the flow over the lower surface of the airfoil at this angle of attack. The latter factor was discussed when considering the angle of attack for zero lift. Since the greater proportion of the profile drag at zero lift is friction drag, the decrease with Reynolds Number is to be expected. The manner in which the friction drag of flat plates changes with the Reynolds Number has been subjected to the most complete theoretical and experimental study, and a comprehensive review of the subject is given in reference 10. Figure 13 presents the drag curve of the flat plate with completely turbulent boundary layer from this reference. The profile-drag coefficients at zero lift from the present airfoil tests are also shown on this curve. These coefficients have been reduced to the same form as those for the flat plate by using the true surface area of the airfoil in the drag equation. The values for the airfoils lie above those for the flat plate with completely turbulent boundary layer, and the shape of the curve suggests that it might lie on one of the intermediate transition curves between those for the laminar and turbulent flow if the pressure drag were deducted.

The profile-drag coefficients calculated from the results of airfoil tests in the propeller-research and variable-density tunnels are presented in figure 12, and their values are in fair agreement. The propeller-research-tunnel value is within the experimental scattering of the points from the full-scale tunnel; the variable-density-tunnel value is only slightly higher. The variable-density-tunnel value for an airfoil with the corresponding thickness and camber taken from the results of tests on related airfoil (reference 6) has been given rather than the results from an earlier test on a Clark Y airfoil, because the more recent tests are believed to be more accurate.

A characteristic of great interest to the designer is the profile-drag coefficient at the lift coefficient for maximum speed. These high-speed lift coefficients usually lie in a range from about C_L=0.1 to 0.2, and the values of the profile-drag coefficient for these two lift coefficients are plotted against Reynolds Number in figure 14. These curves have the same general characteristics as the drag at zero lift.

The pitching-moment coefficient at zero lift (fig. 15) does not change with increase in scale, which indicates that the pressure distribution along the chord does not vary greatly with the Reynolds Number. The maximum L/D values (fig. 16) show a considerable scattering of results. For the three Clark Y airfoils no definite change in maximum L/D ratio with Reynolds Number was observed.

CONCLUDING REMARKS

The appreciable variations of Clark Y characteristics with Reynolds Number have their greatest significance in reemphasizing the importance of a more complete and thorough knowledge of the scale effect on all airfoil sections. Results of tests that have already been conducted in the variable-density tunnel indicate that thin, medium, and thick airfoils with different cambers respond differently to changes in scale.

The appreciable effects of turbulence are shown, by comparison of data from the full-scale and variable-density tunnels, to be equally as important as Reynolds Number effect and, for this reason, make the formation of rules or formulas for transforming small-tunnel data to the equivalent full-scale results questionable until further large- and small-scale information is available on the effects of turbulence on a number of airfoil sections. A program for continuing the study of the effects of scale and turbulence upon the characteristics of air-foils has been planned for both the variable-density and full-scale tunnels and has already been started in the variable-density tunnel.

In general, it may be stated that a complete quantitative evaluation of the factors that are the sources of experimental discrepancy must be made for each wind tunnel before correlation and standardization of wind-tunnel data to a flight basis can be effected.

LANGLEY MEMORIAL AERONAUTICAL LABORATORY,
NATIONAL ADVISORY COMMITTEE FOR AERONAUTICS,
LANGLEY FIELD, VA., *June 14, 1934.*

REFERENCES

1. Theodorsen, Theodore, and Silverstein, Abe: Experimental Verification of the Theory of Wind-Tunnel Boundary Interference. T.R. No. 478, N.A.C.A., 1934.
2. DeFrance, Smith J.: The N.A.C.A. Full-Scale Wind Tunnel. T.R. No. 459, N.A.C.A., 1933.
3. Wood, Donald H.: Tests of Large Airfoils in the Propeller Research Tunnel, Including Two with Corrugated Surfaces. T.R. No. 336, N.A.C.A., 1929.
4. Stack, John: Tests in the Variable Density Wind Tunnel to Investigate the Effects of Scale and Turbulence on Airfoil Characteristics. T.N. No. 364, N.A.C.A., 1931.
5. Garrick, I. E.: Determination of the Theoretical Pressure Distribution for Twenty Airfoils. T.R. No. 465, N.A.C.A., 1933.
6. Jacobs, Eastman N., Ward, Kenneth E., and Pinkerton, Robert M.: The Characteristics of 78 Related Airfoil Sections from Tests in the Variable-Density Wind Tunnel. T.R. No. 460, N.A.C.A., 1933.
7. von Kármán, Th.: Quelques Problèmes Actuels de L'Aérodynamique. Paper read before Journées Techniques Internationales de L'Aéronautique, Chambre Syndicale des Industries Aéronautiques, Dec. 1, 1932.
8. Millikan, C. B., and Klein, A. L.: The Effect of Turbulence. Aircraft Engineering, August 1933, pp. 169–174.
9. Dryden, Hugh L.: Reduction of Turbulence in Wind Tunnels. T.R. No. 392, N.A.C.A., 1931.
10. von Kármán, Th.: Turbulence and Skin Friction. Jour. of the Aero. Sciences vol. I, no. 1, January 1934, pp. 1–20.

TABLE I

SPECIFIED AND AVERAGE MEASURED ORDINATES OF THE CLARK Y AIRFOILS

Distance from leading edge in percent of chord	Standard ordinates in percent of chord		4- by 24-foot				6- by 36-foot				8- by 48-foot			
			Upper surface		Lower surface		Upper surface		Lower surface		Upper surface		Lower surface	
	Upper surface	Lower surface	Specified inches	Average measured inches	Specified inches	Average measured inches	Specified inches	Average measured inches	Specified inches	Average measured inches	Specified inches	Average measured inches	Specified inches	Average measured inches
0	3.50	3.50	1.68	--------	1.68	--------	2.52	--------	2.52	--------	3.36	--------	3.36	--------
1.25	5.45	1.93	2.62	2.63	.93	0.92	3.92	3.92	1.39	1.39	5.23	5.25	1.85	1.85
2.5	6.50	1.47	3.12	3.11	.71	.68	4.68	4.67	1.06	1.05	6.24	6.26	1.41	1.40
5	7.90	.93	3.79	3.77	.45	.43	5.69	5.69	.67	.66	7.58	7.58	.90	.89
7.5	8.85	.63	4.25	4.24	.30	.29	6.37	6.37	.45	.45	8.52	8.52	.60	.61
10	9.60	.42	4.61	4.60	.20	.20	6.91	6.92	.30	.30	9.21	9.22	.40	.40
15	10.68	.15	5.13	5.13	.07	.08	7.69	7.71	.11	.12	10.26	10.26	.14	.14
20	11.36	.03	5.45	5.43	.01	.02	8.18	8.20	.02	.05	10.91	10.91	.03	.02
30	11.70	.00	5.62	5.61	.00	.00	8.42	8.48	.00	.01	11.23	11.25	.00	.00
40	11.40	.00	5.47	5.46	.00	.00	8.21	8.25	.00	.00	10.94	10.95	.00	.00
50	10.52	.00	5.05	5.04	.00	.00	7.57	7.61	.00	.01	10.09	10.11	.00	.00
60	9.15	.00	4.39	4.38	.00	.00	6.59	6.64	.00	.01	8.78	8.78	.00	.00
70	7.35	.00	3.53	3.52	.00	.00	5.29	5.36	.00	.02	7.05	7.06	.00	.00
80	5.22	.00	2.51	2.50	.00	.00	3.76	3.84	.00	.02	5.01	5.02	.00	.00
90	2.80	.00	1.34	1.34	.00	.00	2.02	2.08	.00	.01	2.69	2.68	.00	.00
95	1.49	.00	.72	.71	.00	−.01	1.08	1.14	.00	.01	1.43	1.42	.00	.00
100	.12	.00	.06	--------	.00	--------	.09	.11	.00	.02	.12	.09	.00	−.02

TABLE II

4 BY 24 CLARK Y AIRFOIL CHARACTERISTICS
R.N.: ZERO LIFT=1.12×10^6, MAX. LIFT=1.07×10^6

C_L	α	C_D	L/D	c.p.	$C_{m_{c/4}}$	C_{D_0}	α
−0.2	−9.0°	0.0120	−16.7	−11.1	−0.072	0.0098	−8.3°
−.1	−7.7	.0100	−10.0	−44.7	−.070	.0094	−7.3
0	−6.2	.0097	0		−.068	.0096	−6.2
.1	−4.8	.0102	9.8	93.8	−.068	.0096	−5.2
.2	−3.3	.0120	16.7	58.7	−.067	.0098	−4.0
.3	−1.9	.0155	19.6	48.0	−.066	.0103	−3.0
.4	−.5	.0200	20.0	41.2	−.065	.0111	−1.9
.5	.9	.0254	19.7	38.0	−.065	.0115	−.9
.6	2.3	.0320	18.8	35.8	−.065	.0120	.2
.7	3.7	.0392	17.9	34.1	−.064	.0119	1.2
.8	5.2	.0493	16.2	32.7	−.062	.0137	2.3
.9	6.7	.0600	15.0	31.5	−.059	.0150	3.5
1.0	8.3	.0738	13.7	30.6	−.056	.0181	4.7
1.1	10.1	.0901	12.2	29.8	−.053	.0227	6.2
1.2	12.0	.1092	11.0	29.2	−.050	.0290	7.7
1.227	13.0	.1240	9.9	30.1	−.062	.0415	8.6
1.2	14.4	.1560	7.7	31.7	−.081	.0758	10.1
1.1	17.2	.2160	5.1	33.3	−.092	.1486	13.3
1.0	20.2	.2769	3.6	34.7	−.100	.2202	16.6
.9	20.7	.3388	2.7	36.7	−.113	.2938	17.5
.8	22.5	.3860	2.1	40.0	−.133	.3504	19.6

TABLE III

4 BY 24 CLARK Y AIRFOIL CHARACTERISTICS
R.N.: ZERO LIFT=1.55×10^6, MAX. LIFT=1.48×10^6

C_L	α	C_D	L/D	c.p.	$C_{m_{c/4}}$	C_{D_0}	α_0
−0.2	−9.0°	0.0120	−16.7	−13.1	−0.076	0.0098	−8.4°
−.1	−7.7	.0099	−10.1	−50.7	−.076	.0093	−7.3
0	−6.2	.0092	0		−.076	.0088	−6.2
.1	−4.9	.0093	10.8	99.9	−.074	.0087	−5.3
.2	−3.4	.0112	17.9	61.7	−.073	.0090	−4.1
.3	−2.0	.0145	20.7	48.7	−.071	.0095	−3.1
.4	−.6	.0192	20.8	42.0	−.068	.0103	−2.0
.5	.8	.0242	20.6	38.0	−.065	.0103	−1.0
.6	2.2	.0312	19.2	35.6	−.064	.0112	.1
.7	3.6	.0395	17.9	33.8	−.062	.0122	1.1
.8	5.0	.0485	16.5	32.7	−.062	.0129	2.1
.9	6.4	.0582	15.5	31.9	−.062	.0132	3.2
1.0	7.9	.0700	14.3	31.2	−.062	.0143	4.3
1.1	9.6	.0860	12.8	30.7	−.063	.0186	5.7
1.2	11.7	.1093	11.0	30.3	−.064	.0291	7.4
1.255	13.7	.1540	8.1	31.0	−.075	.0664	9.2
1.2	16.4	.2118	5.7	32.8	−.094	.1316	12.1
1.1	19.4	.2660	4.1	34.5	−.107	.1986	15.5
1.0	20.4	.2900	3.5	36.4	−.118	.2343	16.8
.9	20.9	.3039	3.0	38.3	−.128	.2589	17.7

TABLE IV

4 BY 24 CLARK Y AIRFOIL CHARACTERISTICS
R.N.: ZERO LIFT=2.06×10^6, MAX. LIFT=1.96×10^6

C_L	α	C_D	L/D	c.p.	$C_{m_{c/4}}$	C_{D_0}	α_0
−0.2	−8.8°	0.0116	−17.2	−13.1	−0.076	0.0094	−8.1°
−.1	−7.4	.0095	−10.5	−49.7	−.075	.0089	−7.0
0	−6.0	.0090	0		−.074	.0090	−6.0
.1	−4.6	.0099	10.1	99.8	−.074	.0093	−5.0
.2	−3.2	.0118	16.9	61.7	−.073	.0096	−3.9
.3	−1.8	.0151	19.9	49.0	−.072	.0101	−2.9
.4	−.4	.0197	20.3	42.5	−.070	.0108	−1.8
.5	1.0	.0255	19.6	39.0	−.070	.0116	−.8
.6	2.4	.0325	18.5	36.5	−.069	.0125	.3
.7	3.8	.0404	17.3	34.7	−.068	.0131	1.3
.8	5.0	.0490	16.3	33.4	−.067	.0134	2.4
.9	6.7	.0612	14.7	32.3	−.066	.0162	3.5
1.0	8.2	.0749	13.4	31.5	−.065	.0192	4.6
1.1	9.8	.0901	12.2			.0227	5.9

TABLE V

4 BY 24 CLARK Y AIRFOIL CHARACTERISTICS
R.N.: ZERO LIFT=2.81×10^6, MAX. LIFT=2.62×10^6

C_L	α	C_D	L/D	c.p.	$C_{m_{c/4}}$	C_{D_0}	α_0
−0.2	−8.5°	0.0110	−18.3	−13.6	−0.077	0.0088	−7.8°
−.1	−7.2	.0098	−10.2	−51.7	−.077	.0090	−6.8
0	−5.8	.0089	0		−.077	.0090	−5.8
.1	−4.4	.0100	10.0	100.8	−.075	.0094	−4.8
.2	−3.0	.0120	16.7	62.2	−.074	.0098	−3.7
.3	−1.6	.0157	19.1	49.0	−.072	.0107	−2.7
.4	−.2	.0201	19.9	42.5	−.070	.0112	−1.6
.5	1.2	.0265	18.9	38.4	−.067	.0126	−.6
.6	2.5	.0330	18.0	36.1	−.067	.0130	.4
.7	3.9	.0411	17.0	34.7	−.068	.0138	1.4
.8	5.3	.0507	15.8	33.5	−.068	.0151	2.4
.9	6.8	.0620	14.5	32.5	−.068	.0170	3.6
1.0	8.2	.0749	13.4	31.5	−.065	.0192	4.6
1.1	9.8	.0901	12.2	30.8	−.064	.0227	5.9
1.2	11.5	.1082	11.1	30.3	−.063	.0280	7.2
1.3	13.1	.1260	10.4	29.9	−.063	.0318	8.5
1.370	14.4	.1405	9.7	29.9	−.067	.0360	9.5
1.3	16.4	.2015	6.5	31.5	−.085	.1073	11.8
1.2	17.4	.2260	5.3	32.2	−.087	.1458	13.1
1.1	20.0	.2788	3.9	33.9	−.100	.2114	16.1
1.0	22.1	.3260	3.1	36.2	−.116	.2703	18.5

TABLE VI

4 BY 24 CLARK Y AIRFOIL CHARACTERISTICS
R.N.: ZERO LIFT=3.19×10^6, MAX. LIFT=2.96×10^6

C_L	α	C_D	L/D	c.p.	$C_{m_{c/4}}$	C_{D_0}	α_0
−0.2	−8.5°	0.0100	−20.0	−15.1	−0.080	0.0089	−7.8°
−.1	−7.1	.0095	−10.5	−52.7	−.078	.0089	−6.7
0	−5.7	.0089	0		−.077	.0089	−5.7
.1	−4.3	.0095	10.5	100.8	−.075	.0089	−4.7
.2	−2.9	.0118	17.0	62.2	−.074	.0096	−3.6
.3	−1.5	.0155	19.4	49.0	−.072	.0105	−2.6
.4	−.1	.0202	19.8	42.5	−.070	.0113	−1.5
.5	1.3	.0270	18.5	38.6	−.068	.0131	−.5
.6	2.7	.0345	17.4	36.3	−.068	.0145	.6
.7	4.0	.0425	16.5	34.7	−.068	.0152	1.5
.8	5.4	.0525	15.2	33.4	−.067	.0169	2.5
.9	6.9	.0638	14.1	32.4	−.067	.0183	3.7
1.0	8.2	.0755	13.2	31.6	−.066	.0198	4.6
1.1	9.8	.0900	12.2	30.9	−.065	.0226	5.9
1.2	11.3	.1055	11.3	30.0	−.060	.0253	7.0
1.3	13.1	.1261	10.3	29.5	−.058	.0319	8.5
1.381	14.9	.1482	9.3	30.1	−.070	.0419	10.0
1.3	15.0	.1600	8.1	31.0	−.078	.0658	10.4
1.2	18.1	.2400	5.0	32.4	−.090	.1598	13.8
1.1	20.7	.2900	3.8	34.4	−.106	.2226	16.8
1.0	22.7	.3395	2.9	35.5	−.111	.2838	19.1

TABLE VII

4 BY 24 CLARK Y AIRFOIL CHARACTERISTICS
R.N.: ZERO LIFT=3.59×10^6, MAX. LIFT=3.50×10^6

C_L	α	C_D	L/D	c.p.	$C_{m_{c/4}}$	C_{D_0}	α_0
−0.2	−8.4°	0.0108	−18.5	−13.0	−0.075	0.0086	−7.7°
−.1	−7.0	.0094	−10.6	−49.7	−.075	.0088	−6.6
0	−5.6	.0087	0		−.075	.0089	−5.6
.1	−4.2	.0094	10.6	99.7	−.074	.0088	−4.6
.2	−2.8	.0117	17.1	61.6	−.073	.0090	−3.5
.3	−1.4	.0150	20.0	49.0	−.072	.0100	−2.5
.4	0	.0199	20.1	42.8	−.071	.0110	−1.4
.5	1.4	.0260	19.2	39.0	−.070	.0121	−.4
.6	2.8	.0338	17.8	36.3	−.068	.0138	.7
.7	4.1	.0420	16.7	34.6	−.067	.0153	1.6
.8	5.6	.0530	15.1	33.2	−.066	.0174	2.7
.9	7.0	.0641	14.1	32.2	−.065	.0191	3.8
1.0	8.4	.0770	13.0	31.4	−.064	.0213	4.8
1.1	10.0	.0920	11.9	30.7	−.063	.0246	6.1
1.2	11.5	.1080	11.1	30.2	−.062	.0278	7.2
1.3	13.1	.1260	10.3	29.6	−.060	.0318	8.5
1.4	14.7	.1461	9.6	29.3	−.060	.0371	9.7
1.420	15.2	.1528	9.3	29.5	−.064	.0406	10.1
1.4	15.5	.1575	8.9	29.8	−.067	.0485	10.5
1.3	18.5	.2434	5.3	32.6	−.100	.1492	13.9
1.2	19.4	.2698	4.4	34.0	−.100	.1896	15.1
1.1	20.8	.2982	3.7	36.2	−.116	.2308	16.9
1.0	23.2	.3355	3.0	36.2	−.118	.2798	19.6

TABLE VIII

6 BY 36 CLARK Y AIRFOIL CHARACTERISTICS
R.N.: ZERO LIFT=2.07×10^6, MAX. LIFT=1.90×10^6

C_L	α	C_D	L/D	[1] c.p.	[1] $C_{m_{c/4}}$	C_{D_0}	α_0
−0.1	−7.0°	0.0110	−9.0	--------	--------	0.0105	−6.6°
0	−5.7	.0100	0	--------	--------	.0100	−5.7
.1	−4.3	.0102	9.8	--------	--------	.0096	−4.7
.2	−2.8	.0117	17.1	--------	--------	.0091	−3.5
.3	−1.3	.0145	20.7	--------	--------	.0095	−2.6
.4	−.1	.0189	21.2	--------	--------	.0092	−1.5
.5	1.3	.0234	21.4	--------	--------	.0095	−.5
.6	2.7	.0300	20.0	--------	--------	.0100	.6
.7	4.0	.0382	18.3	--------	--------	.0109	1.5
.8	5.4	.0476	16.8	--------	--------	.0120	2.5
.9	6.9	.0591	15.2	--------	--------	.0134	3.7
1.0	8.3	.0708	14.1	--------	--------	.0151	4.7
1.1	10.1	.0863	12.7	--------	--------	.0179	6.0
1.2	11.7	.1020	11.8	--------	--------	.0218	7.4
1.285	13.6	.1264	10.2	--------	--------	.0344	9.0
1.2	18.1	.2265	5.3	--------	--------	.1463	13.8
1.1	19.7	.2606	4.2	--------	--------	.1932	15.8
1.0	21.5	.3081	3.2	--------	--------	.2534	17.9

[1] Not measured.

TABLE IX

6 BY 36 CLARK Y AIRFOIL CHARACTERISTICS
R.N.: ZERO LIFT=3.04×10^6, MAX. LIFT=2.75×10^6

C_L	α	C_D	L/D	c.p.	$C_{m_{c/4}}$	C_{D_0}	α_0
−0.1	−6.9°	0.0098	−10.4	−54.7	−0.080	0.0090	−6.5°
0	−5.6	.0088	0	--------	−.077	.0088	−5.6
.1	−4.2	.0093	10.8	99.7	−.074	.0087	−4.6
.2	−2.8	.0112	17.8	59.2	−.068	.0090	−3.5
.3	−1.4	.0145	20.7	47.3	−.067	.0095	−2.5
.4	0	.0189	21.2	41.2	−.065	.0100	−1.4
.5	1.4	.0239	20.9	37.8	−.064	.0100	−.4
.6	2.8	.0310	19.4	35.8	−.062	.0110	.7
.7	4.1	.0387	18.1	33.7	−.061	.0114	1.6
.8	5.6	.0476	16.8	32.2	−.058	.0120	2.7
.9	7.0	.0585	15.4	31.3	−.057	.0130	3.8
1.0	8.3	.0697	14.3	30.6	−.056	.0145	4.7
1.1	10.0	.0843	13.0	29.8	−.058	.0163	6.1
1.2	11.5	.0990	12.1	29.2	−.050	.0188	7.2
1.3	13.3	.1180	11.0	23.8	−.049	.0238	8.7
1.330	14.2	.1307	10.2	28.9	−.052	.0322	9.5
1.3	14.7	.1485	8.8	30.0	−.065	.0543	10.1
1.2	18.9	.2440	4.9	32.2	−.087	.1638	14.6
1.1	20.7	.2828	3.9	34.2	−.104	.2154	16.8
1.0	22.0	.3295	3.0	36.2	−.117	.2838	18.4

TABLE X

6 BY 36 CLARK Y AIRFOIL CHARACTERISTICS
R.N.: ZERO LIFT=3.64×10^6, MAX. LIFT=3.22×10^6

C_L	α	C_D	L/D	c.p.	$C_{m_{c/4}}$	C_{D_0}	α_0
−0.1	−6.9°	0.0101	−9.9	−57.6	−0.083	0.0095	−6.5°
0	−5.5	.0090	0	--------	−.080	.0090	−5.5
.1	−4.2	.0095	10.5	103.8	−.078	.0089	−4.6
.2	−2.7	.0112	17.9	62.6	−.075	.0090	−3.4
.3	−1.3	.0145	20.7	48.7	−.071	.0095	−2.4
.4	.1	.0194	20.6	42.0	−.068	.0098	−1.3
.5	1.5	.0246	20.3	38.0	−.065	.0107	−.3
.6	2.8	.0312	19.2	35.5	−.063	.0112	.7
.7	4.2	.0396	17.7	33.7	−.061	.0123	1.7
.8	5.7	.0491	16.3	32.5	−.060	.0134	2.8
.9	7.0	.0585	15.4	31.7	−.060	.0140	3.8
1.0	8.4	.0708	14.1	31.0	−.060	.0147	4.8
1.1	9.9	.0828	13.3	30.5	−.060	.0154	6.0
1.2	11.4	.0978	12.3	30.0	−.060	.0176	7.1
1.3	13.0	.1155	11.3	29.3	−.056	.0213	8.4
1.36	14.7	.1383	9.8	29.0	−.055	.0353	9.8
1.3	15.0	.1555	8.4	29.7	−.061	.0618	10.4
1.2	19.2	.2545	4.7	33.4	−.102	.1743	14.9
1.1	21.6	.3033	3.6	35.2	−.115	.2359	17.7

TABLE XI

6 BY 36 CLARK Y AIRFOIL CHARACTERISTICS
R.N.: ZERO LIFT=4.15×10^6, MAX. LIFT=3.64×10^6

C_L	α	C_D	L/D	c.p.	$C_{m_{c/4}}$	C_{D_0}	α_0
−0.2	−8.4°	--------	--------	--------	--------	--------	−7.7°
−.1	−6.9	0.0098	−10.2	−58.6	−0.084	0.0092	−6.5
0	−5.6	.0088	0	--------	−.080	.0088	−5.6
.1	−4.2	.0094	10.6	102.8	−.077	.0088	−4.6
.2	−2.7	.0111	18.0	62.6	−.075	.0089	−3.4
.3	−1.3	.0145	20.7	49.4	−.073	.0095	−2.4
.4	.1	.0191	20.9	42.2	−.069	.0102	−1.3
.5	1.5	.0243	20.6	38.2	−.066	.0104	−.3
.6	2.9	.0318	19.2	35.5	−.063	.0113	.8
.7	4.2	.0388	18.1	33.8	−.062	.0115	1.7
.8	5.7	.0478	16.7	32.7	−.062	.0122	2.8
.9	7.1	.0585	15.4	31.8	−.061	.0135	3.9
1.0	8.5	.0701	14.3	31.0	−.060	.0144	4.9
1.1	10.1	.0841	13.1	30.3	−.058	.0160	6.2
1.2	11.6	.0989	12.1	29.8	−.057	.0187	7.3
1.3	13.3	.1167	11.1	29.3	−.055	.0225	8.7
1.371	15.0	.1382	9.9	30.4	−.073	.0334	10.1
1.3	15.6	.1695	7.7	29.8	−.062	.0753	11.0
1.2	18.5	.2338	5.1	32.4	−.090	.1536	14.2
1.1	21.2	.2858	3.8	34.1	−.102	.2184	17.3

TABLE XII

6 BY 36 CLARK Y AIRFOIL CHARACTERISTICS
R.N.: ZERO LIFT=4.77×10^6, MAX. LIFT=4.20×10^6

C_L	α	C_D	L/D	c.p.	$C_{m_{c/4}}$	C_{D_0}	α_0
−0.2	−8.2°	0.0122	−16.4	−18.6	−0.087	0.0100	−7.5°
−.1	−6.8	.0101	−9.9	−54.6	−.080	.0095	−6.4
0	−5.6	.0089	0	--------	−.076	.0089	−5.6
.1	−4.1	.0093	10.7	98.7	−.073	.0087	−4.5
.2	−2.7	.0110	18.2	60.1	−.070	.0088	−3.4
.3	−1.4	.0140	21.4	47.4	−.067	.0090	−2.5
.4	−.1	.0186	21.5	41.3	−.065	.0097	−1.5
.5	1.4	.0234	21.4	37.8	−.064	.0095	−.4
.6	2.6	.0300	20.0	35.5	−.063	.0100	.5
.7	3.9	.0376	18.6	33.7	−.061	.0103	1.4
.8	5.4	.0475	16.8	32.5	−.060	.0119	2.5
.9	6.7	.0570	15.8	31.7	−.060	.0120	3.5
1.0	8.0	.0676	14.8	31.0	−.060	.0119	4.4
1.1	9.4	.0798	13.8	30.3	−.058	.0124	5.5
1.2	10.8	.0935	12.9	29.7	−.056	.0133	6.5
1.3	12.4	.1096	11.9	29.1	−.053	.0154	7.8
1.4	14.3	.1299	10.8	28.7	−.052	.0209	9.3
1.448	15.6	.1483	9.8	29.3	−.062	.0313	10.4
1.4	15.8	.1530	9.2	29.8	−.067	.0440	10.8
1.3	16.0	.1815	7.2	30.3	−.069	.0873	11.4
1.2	19.6	.2675	4.5	33.1	−.099	.2593	15.3
1.1	22.8	.3396	3.2	34.3	−.106	.2722	18.9

TABLE XIII

6 BY 36 CLARK Y AIRFOIL CHARACTERISTICS
R.N.: ZERO LIFT=5.86×10^6

C_L	α	C_D	L/D	c.p.	$C_{m_{c/4}}$	C_{D_0}	α_0
−0.1	−6.9°	0.0097	10.3	−56.5	−0.082	0.0091	−6.5°
0	−5.5	.0090	0	--------	−.077	.0090	−5.5
.1	−4.4	.0094	10.6	98.7	−.073	.0088	−4.5
.2	−2.6	.0112	17.9	60.1	−.070	.0090	−3.3
.3	−1.2	.0147	20.4	47.7	−.068	.0097	−2.2
.4	.2	.0200	20.0	41.8	−.067	.0111	−1.2
.5	1.7	.0254	19.7	38.0	−.065	.0115	−.1
.6	3.1	.0322	18.6	35.6	−.064	.0122	1.0
.7	4.3	.0402	17.4	34.0	−.063	.0129	2.0
.8	5.8	.0496	16.2	32.9	−.063	.0140	3.0

TABLE XIV

8 BY 48 CLARK Y AIRFOIL CHARACTERISTICS
R.N.: ZERO LIFT=2.20×10⁶, MAX. LIFT=1.84×10⁶

C_L	α	C_D	L/D	c.p.	$C_{m_{c/4}}$	C_{D_0}	α_0
−0.2	−8.4°	0.0131	−15.3	−15.6	−0.081	0.0109	−7.7°
−.1	−7.0	.0108	−9.3	−52.5	−.078	.0103	−6.6
0	−5.6	.0099	0		−.075	.0099	−5.6
.1	−4.2	.0099	10.1	98.7	−.073	.0093	−4.5
.2	−2.8	.0110	18.2	60.6	−.071	.0088	−3.6
.3	−1.4	.0134	22.4	48.4	−.070	.0084	−2.5
.4	0	.0175	22.9	42.5	−.070	.0086	−1.4
.5	1.4	.0230	21.7	38.8	−.069	.0091	−.4
.6	2.7	.0305	19.7	36.3	−.068	.0104	.5
.7	4.1	.0387	18.1	34.4	−.066	.0114	1.6
.8	5.5	.0483	16.6	33.1	−.065	.0127	2.7
.9	7.0	.0590	15.3	32.2	−.065	.0139	3.8
1.0	8.6	.0721	13.9	31.5	−.065	.0164	5.0
1.1	10.2	.0876	12.6	30.7	−.063	.0202	6.3
1.2	11.9	.1040	11.5	30.2	−.062	.0238	7.6
1.3	13.7	.1232	10.5	29.8	−.062	.0291	9.0
1.325	14.7	.1399	9.5	30.0	−.066	.0420	10.0
1.3	15.8	.1644	7.9	31.0	−.078	.0703	11.2
1.2	17.7	.2133	5.6	33.0	−.096	.1331	13.4
1.1	19.6	.2591	4.2	35.0	−.112	.1917	15.6
1.0	21.9	.3191	3.1	37.0	−.125	.2635	18.3

TABLE XV

8 BY 48 CLARK Y AIRFOIL CHARACTERISTICS
R.N.: ZERO LIFT=3.10×10⁶, MAX. LIFT=2.59×10⁶

C_L	α	C_D	L/D	c.p.	$C_{m_{c/4}}$	C_{D_0}	α_0
−0.2	−8.3°	0.0130	−15.4	−17.0	−0.084	0.0108	−7.6°
−.1	−7.0	.0101	−9.9	−54.6	−.080	.0095	−6.6
0	−5.5	.0091	0		−.075	.0091	−5.5
.1	−4.1	.0093	10.8	98.7	−.073	.0087	−4.5
.2	−2.7	.0106	18.9	60.1	−.070	.0084	−3.4
.3	−1.3	.0131	22.9	48.0	−.069	.0081	−2.4
.4	.1	.0180	22.2	41.8	−.067	.0091	−1.3
.5	1.5	.0234	21.4	38.4	−.067	.0095	−.4
.6	2.8	.0305	19.7	36.2	−.067	.0104	.7
.7	4.2	.0389	18.0	34.5	−.067	.0116	1.7
.8	5.6	.0481	16.6	33.4	−.067	.0125	2.7
.9	7.0	.0590	15.3	32.4	−.067	.0138	3.8
1.0	8.6	.0721	13.8	31.7	−.067	.0164	5.0
1.1	10.1	.0870	12.7	31.2	−.068	.0196	6.2
1.2	11.8	.1046	11.5	30.6	−.067	.0244	7.5
1.3	13.6	.1228	10.6	30.2	−.067	.0311	8.9
1.36	15.2	.1442	9.4	29.9	−.066	.0413	10.3
1.3	16.4	.1772	7.3	31.9	−.090	.0831	11.8
1.2	18.4	.2333	5.1	33.8	−.106	.1531	14.1
1.1	20.6	.2811	3.9	35.3	−.116	.2137	16.6
1.0	22.8	.3256	3.1	36.5	−.120	.3597	19.3

TABLE XVI

8 BY 48 CLARK Y AIRFOIL CHARACTERISTICS
R.N.: ZERO LIFT=4.13×10⁶, MAX. LIFT=3.78×10⁶

C_L	α	C_D	L/D	c.p.	$C_{m_{c/4}}$	C_{D_0}	α_0
−0.2	−8.2°	0.0126	−15.9	−17.1	−0.084	0.0104	−7.5°
−.1	−6.9	.0100	−10.0	−53.6	−.079	.0094	−6.5
0	−5.5	.0090	0		−.075	.0090	−5.5
.1	−4.1	.0095	10.5	98.7	−.073	.0089	−4.5
.2	−2.8	.0109	18.4	60.6	−.071	.0087	−3.5
.3	−1.4	.0137	21.9	48.4	−.070	.0087	−2.5
.4	0	.0175	22.9	42.5	−.070	.0086	−1.4
.5	1.3	.0228	21.9	39.0	−.070	.0089	−.5
.6	2.6	.0295	20.3	36.5	−.069	.0094	.5
.7	4.0	.0377	18.6	34.8	−.069	.0104	1.5
.8	5.3	.0465	17.2	33.5	−.068	.0109	2.5
.9	6.7	.0573	15.7	32.6	−.068	.0122	3.5
1.0	8.2	.0690	14.5	31.8	−.068	.0133	4.6
1.1	9.6	.0824	13.3	31.1	−.067	.0150	5.7
1.2	11.2	.0998	12.0	30.5	−.066	.0196	6.9
1.3	12.8	.1182	11.0	30.0	−.065	.0241	8.2
1.4	14.7	.1398	10.0	29.7	−.065	.0306	9.7
1.445	15.9	.1550	9.3	30.2	−.075	.0387	10.7
1.4	17.4	.2058	6.8	30.4	−.075	.0966	12.4
1.3	19.0	.2492	5.2	32.3	−.095	.1551	14.4
1.2	21.6	.2832	4.2	34.8	−.120	.2304	17.3

TABLE XVII

8 BY 48 CLARK Y AIRFOIL CHARACTERISTICS
R.N.: ZERO LIFT=5.58×10⁶, MAX. LIFT=4.43×10⁶

C_L	α	C_D	L/D	c.p.	$C_{m_{c/4}}$	C_{D_0}	α_0
−0.2	−8.1°	0.0119	−16.8	−15.1	−0.080	0.0097	−7.4°
−.1	−6.8	.0098	−10.2	−51.7	−.077	.0092	−6.4
.0	−5.4	.0088	0		−.076	.0088	−5.4
.1	−4.0	.0091	11.0	100.6	−.075	.0085	−4.4
.2	−2.6	.0106	18.9	62.6	−.075	.0084	−3.3
.3	−1.2	.0137	21.9	49.7	−.074	.0087	−2.3
.4	.2	.0183	21.9	43.5	−.074	.0094	−1.3
.5	1.5	.0234	21.4	39.6	−.073	.0095	−.3
.6	2.8	.0303	19.8	36.8	−.071	.0102	.7
.7	4.2	.0282	18.3	35.0	−.070	.0109	1.7
.8	5.5	.0465	17.2	33.6	−.069	.0115	2.6
.9	6.9	.0578	15.6	32.4	−.067	.0127	3.7
1.0	8.3	.0696	14.3	31.5	−.065	.0139	4.7
1.1	9.8	.0831	13.2	31.0	−.066	.0162	5.9
1.2	11.4	.1003	12.0	30.6	−.067	.0201	7.1
1.3	13.0	.1182	11.0	30.2	−.067	.0241	8.4
1.4	14.8	.1388	10.1	30.0	−.069	.0296	9.8
1.46	16.2	.1600	9.1	29.7	−.068	.0413	11.0
1.4	16.9	.1768	7.9	30.0	−.069	.0676	11.9
1.3	17.7	.2190	5.9	31.9	−.090	.1251	13.1
1.2	22.1	.3210	3.7	35.2	−.125	.2406	17.8

TABLE XVIII

8 BY 48 CLARK Y AIRFOIL CHARACTERISTICS
R.N.: ZERO LIFT=6.12×10⁶, MAX. LIFT=5.38×10⁶

C_L	α	C_D	L/D	c.p.	$C_{m_{c/4}}$	C_{D_0}	α_0
−0.2	−8.1°	0.0124	−16.1	−15.0	−0.080	0.0102	−7.4°
−.1	−6.7	.0097	−10.3	−54.0	−.078	.0091	−6.3
.0	−5.3	.0086	0		−.076	.0086	−5.3
.1	−3.9	.0089	10.2	96.1	−.075	.0083	−4.3
.2	−2.6	.0106	18.9	61.9	−.073	.0084	−3.3
.3	−1.3	.0139	21.6	49.5	−.072	.0089	−2.3
.4	.2	.0181	22.1	43.0	−.072	.0092	−1.3
.5	1.5	.0234	21.4	39.5	−.071	.0095	−.3
.6	2.8	.0305	19.7	37.0	−.071	.0104	.7
.7	4.2	.0382	18.3	35.0	−.071	.0109	1.7
.8	5.6	.0476	16.8	34.0	−.071	.0120	2.7
.9	6.9	.0581	15.5	33.0	−.070	.0130	3.7
1.0	8.4	.0696	14.4	32.1	−.070	.0139	4.8
1.1	9.8	.0836	13.2	31.3	−.070	.0162	5.9
1.2	11.3	.0999	12.0	30.9	−.070	.0186	7.0
1.3	12.9	.1170	11.0	30.3	−.070	.0231	8.3
1.4	14.7	.1380	10.1	30.0	−.070	.0286	9.7
1.51	16.7	.1660	9.1	29.9	−.070	.0390	11.3
1.4	17.3	.1910	7.3	29.8	−.066	.0816	12.3
1.3	19.2	.2570	5.1	33.6	−.110	.1631	14.6
1.2	22.0	.3150	3.8	34.9	−.118	.2346	17.7

TABLE XIX

8 BY 48 CLARK Y AIRFOIL CHARACTERISTICS
R.N.: ZERO LIFT=7.53×10⁶

C_L	α	C_D	L/D	c.p.	$C_{m_{c/4}}$	C_{D_0}	α_0
−0.2	−8.3°	0.0126	−15.9	−15.1	−0.080	0.0104	−7.6°
−.1	−6.8	.0097	−10.3	−51.7	−.077	.0091	−6.4
.0	−5.3	.0086	0		−.075	.0086	−5.3
.1	−3.8	.0092	10.9	99.6	−.074	.0086	−4.2
.2	−2.3	.0112	17.9	61.6	−.073	.0090	−3.0
.3	−1.0	.0147	20.4	48.7	−.071	.0097	−2.1
.4	.3	.0183	21.8	42.5	−.070	.0094	−1.2
.5	1.6	.0240	20.8	39.0	−.070	.0101	−.2
.6	2.9	.0305	19.7	36.7	−.070	.0104	.8
.7	4.3	.0385	18.2	35.0	−.070	.0112	1.8
.8	5.6	.0464	17.3	33.9	−.071	.0108	2.7

TABLE XX

8 BY 48 CLARK Y AIRFOIL CHARACTERISTICS
R.N.: ZERO LIFT=8.77×10⁶

C_L	α	C_D	L/D	c.p.	$C_{m_{c/4}}$	C_{D_0}	α_0
−0.1	−7.2°	0.0095	−10.5	−55.7	−0.081	0.0089	−6.8°
.0	−5.4	.0087	0		−.076	.0087	−5.4
.1	−3.7	.0091	11.0	99.6	−.074	.0085	−4.1
.2	−2.3	.0108	18.5	61.6	−.073	.0086	−3.0
.3	−1.0	.0139	21.6	49.0	−.072	.0089	−2.1
.4	.2	.0180	22.2	42.8	−.070	.0091	−1.2
.5	1.5	.0229	21.8	39.2	−.071	.0090	−.3
.6	2.8	.0285	21.6	37.0	−.072	.0084	.6